An algorithm for statistical evaluation of weld toe geometries using laser triangulation

Autors: Finn Renken[1], Rüdiger Ulrich Franz von Bock und Polach[1], Jan Schubnell[2], Matthias Jung[2], Markus Oswald[3], Klemens Rother[3], Sören Ehlers[1], Moritz Braun[1]

[1]*Institute for Ship Structural Design and Analysis, Hamburg University of Technology, Hamburg, Germany*

[2]*Fraunhofer Institute for Mechanics of Materials (IWM), Freiburg, Germany*

[3]*Dept. Mechanical, Automotive and Aerospace Eng., Munich University of Applied Sciences, Munich, Germany*

This article was published in International Journal of Fatigue Volume 149

https://doi.org/10.1016/j.ijfatigue.2021.106293

Highlights:

- Determination of a representative method to evaluate digitalized weld profiles
- Statistical evaluation of the weld toe geometry, i.e. radius and angle
- Determination of stress concentration factors based on artificial neural networks
- Comparison of geometry and stress concentration factors of long and short welds

Abstract:

Commonly, to evaluate the influence of the local weld geometry in fatigue test, small-scale specimens are used, assuming those represent a longer weld adequately. In this study, a comparison between short specimens and a long weld is performed. A method is developed for the statistical evaluation of weld toe radii and angles, stress concentration factors and weld quality classes. The results show a strong sampling rate dependence and lower ISO 5817:2014 weld quality results for higher sampling rates. Comparable results between short specimens and a long weld can be achieved using modal values of the parameters assuming a lognormal distribution.

Keywords: Local toe geometry, stress concentration factor, weld classification, 3-D scans, statistical assessment

Nomenclature:

Variable	Meaning	Unit
$\alpha_{1.12}$	Weld toe angle	°
σ_{max}	Maximum stress	MPa
σ_N	Nominal stress	MPa
a	Throat thickness	mm
a_i	Polynomial coefficient	–
d	Distance between two points	mm
i	Node number	–
K_t	Stress concentration factor	–
$K_{t,b}$	Stress concentration factor for bending	–
$K_{t,t}$	Stress concentration factor for tension	–
$L_{1.10}$	Weld reinforcement of a fillet weld	mm
$L_{1.16}$	Asymmetry of the leg length	mm
$L_{1.19}$	Weld reinforcement of a butt weld	mm
$L_{1.20}$	To small throat thickness	mm
$L_{1.21}$	To large throat thickness	mm
$L_{1.7}$	Depth of the undercut	mm
n	Total node number	–
R	Radius	mm
S	Number of slices	–
t	Cord length	mm
x	x-coordinate	mm

x'	Spatial derivatives of *x* with respect to *t*	–
x_m	x-coordinate of the centre of the circle	mm
y	y-coordinate	mm
y'	Spatial derivatives of *y* with respect to *t*	–
y_m	y-coordinate of the centre of the circle	mm
z_1	Bottom leg length	mm
z_2	Top leg length	mm

1 Introduction

For fatigue analysis the local geometry of the weld toe is an important factor. In welded constructions the weld reinforcement leads to a stress concentration which affects the fatigue behaviour [1, 2]. Especially high strength steels are sensitive to notches and lose their strength potential under cyclic loading compared to the base material [3, 4]. Accordingly, the local geometry at the weld toe has a great influence for high strength steels. The geometry is mostly affected by the welding technique, shop floor position, weld type and by the welding parameters [5-9]. A sharp weld toe or even undercut reduces the fatigue strength [9-11]. The importance of the weld toe geometry can be seen on different post weld treatments to modify the weld toe geometry [12-14]. This shows how significant the weld toe geometry is.

To investigate the impact of the weld toe geometry, a reliable measurement method of the weld toe is necessary. This measurement method can be done manually or computer-aided based on the digitized surface geometry. A problem with manual procedures is that the result highly differ between users [15]. For this reason, a computer-aided procedure is much more efficient. Examples for computer-aided measurement systems can be found in [4, 16-19]. Important parameters for the fatigue behaviour are the weld toe radius and the flank angle [20-22]. Other investigations also show a high influence of the weld leg length [23]. The stress concentration factor represents local stress concentration at the weld toe and can be estimated from weld toe radius and flank angle [24-26].

A computer-aided measurement method is usually based on a 2D profile of the weld. As a challenge the weld toe geometry is not constant along the weld [27]. Therefore, a common approach is to analyze the weld toe on a specific number of slices along the weld. Small number of slices lead to large scatter of the weld toe parameters, especially for uneven manual weld seams, with a high risk of missing critical areas. Large number of slices, however, need more time for the evaluation which should be avoided if possible.

For fatigue tests small-scale specimens are typically used. However, such short weld seams are rarely used in real structures. Since the geometry changes along the weld seam the question arises whether small-scale specimens are representative for long weld seams. Small-scale specimens only represent a specific section of a weld seam [28]. Thus, the parameters as well as the quality might be different for each specimen. This problem occurs especially with manual welding processes since the weld geometry depends on the user [29]. For this reason, a statistical assessment is required to determine a representative number of slices for each specimen to achieve a comparable result.

In this study a statistical evaluation of a fillet weld in the as-welded condition is conducted by using a computer-aided measurement method to investigate the comparability between short specimens and a longer weld. For this an assessment of the statistical distribution is conducted with respect of the weld parameters. Therefore, a representative number of 2D slices were determined which was used for the comparison between short specimens and long welds. For this comparison a weld seam was separated into four specimens. Each specimen was measured and the results were compared to the longer weld. The considered parameters are the weld radius, weld angle and leg length. With these parameters it is also possible to conduct an evaluation of the stress concentration factor regarding the approach in [24]. In addition to the measuring of the weld toes, a quality assessment according to ISO 5817:2014 [30] is carried out. The aim of this study is to provide a method that permits a statistical evaluation of the local weld geometry and the weld quality along weld seams based on a sensitivity study on sampling rate effects.

2 Measurement of the weld geometry

For reliable and repeatable results, a manual evaluation of the weld geometry is not suitable because of the comparably high effort to create a representative number of measurements

along the weld. To avoid this, a computer-based approach was used. A deterministic program implemented in the commercial software package MATLAB was used for the automatic assessment of the geometrical parameters of the weld toe.

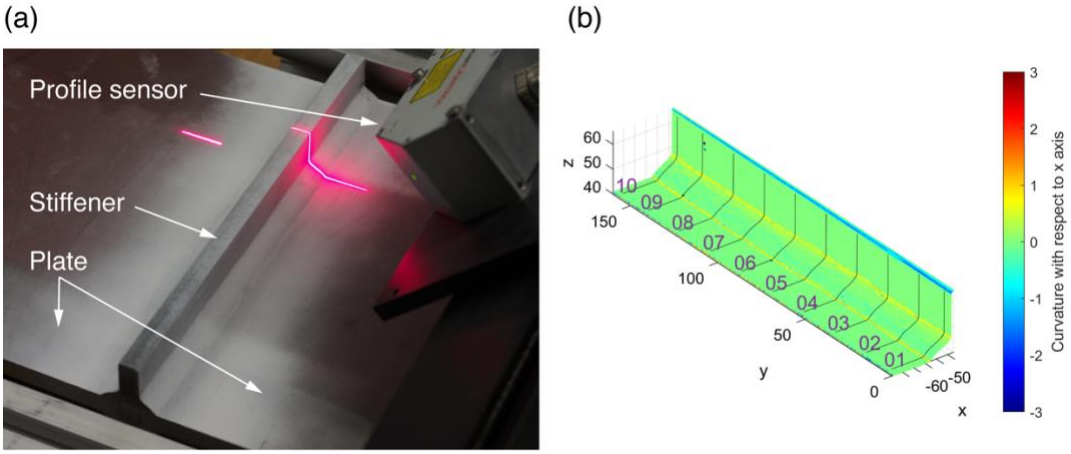

Fig. 1: Laser scanning of specimen (a) and visualization of the welded geometry curvature with ten 2D slices (b)

2.1 Import of the geometry

For the import of the weld geometry a 3D laser scanner with a spatial resolution of about 0.107 mm and a vertical accuracy of 0.01 mm—attached to a carriage on a stiff frame—was used (see Fig. 1 (a)) with supports for specimens' positioning. The scanned geometry (point cloud) was exported as STL-File. Afterwards the point cloud can be exported as an ASCII-file in the x,y,z – coordinates data format. Next, a variable number of 2D slices was extracted from the 3D point cloud (see Fig. 1 (b)).

2.2 Mathematical description of the weld profile

For the geometrical assessment of the 2D weld profile the curvature method was used (see [17, 31]). The curvature in a geometrical context represents the inverse values of the radius and can be comparable easy calculated for each point of a mathematical function. The complex shape of a weld profile cannot be represented by a continuous analytical function. A solution for that is a piecewise polynomial function (spline). A major requirement for the spline algorithm is that the spline passes through all knots to avoid a manipulation of the measured data. Furthermore, it is necessary to represent vertical segments for fillet welds. A cubic parametric spline fulfils these requirements [32]. This spline algorithm is also very suitable for the description of circles [32], which is useful for the evaluation of round weld

toes. The used cubic parametric spline uses the cord length t as the parameter (see Fig. 2(a)).

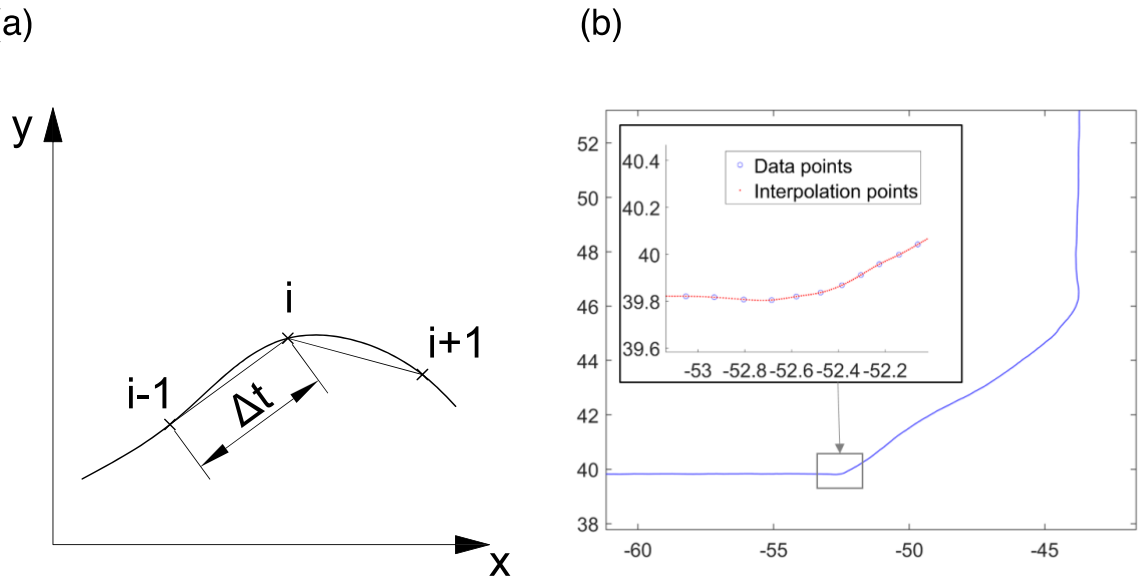

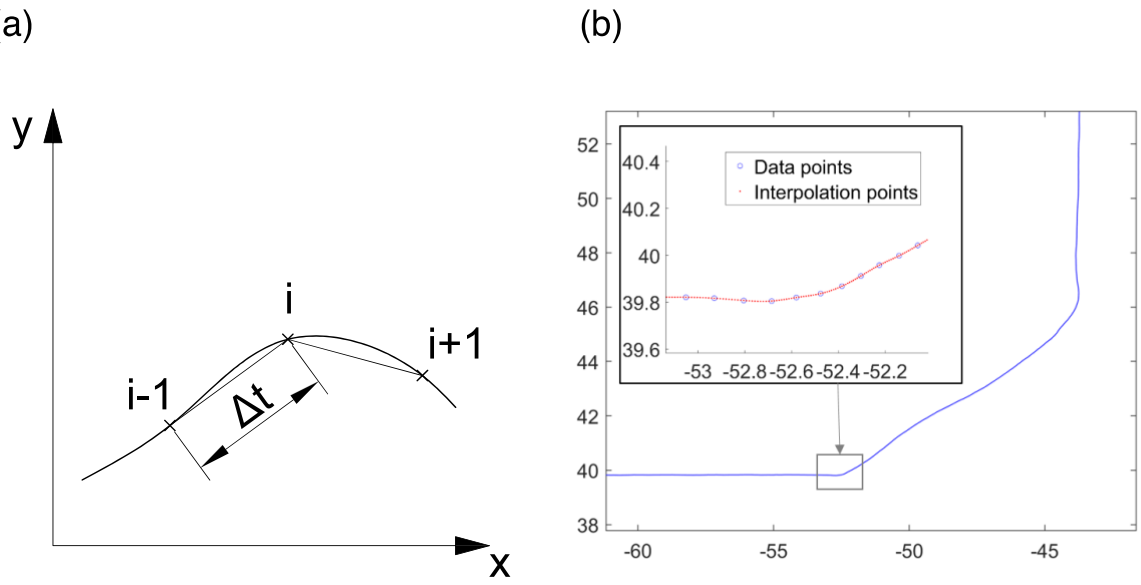

Fig. 2: Parameters of the cubic parametric spline (a) and application to fillet weld with ten interpolated data points (b)

For each segment count the following equations:

$x(t) = a_{3x}t^3 + a_{2x}t^2 + a_{1x}t + a_{0x}$	(2.1)
$y(t) = a_{3y}t^3 + a_{2y}t^2 + a_{1y}t + a_{0y}$	(2.2)

The chord length t is defined as a linear function between the consecutive points:

$t = \sqrt{(x - x_{i-1})^2 + (y - y_{i-1})^2} \qquad , \text{for } 0 \leq t \leq \Delta t$	(2.3)
$\Delta t = \sqrt{(x_i - x_{i-1})^2 + (y_i - y_{i-1})^2}$	(2.4)

From this follow eight unknown polynomial coefficients. They result from the boundary conditions at each node which are constant angle and constant curvature from each segment to another:

$a_{3x} = \frac{1}{\Delta t_i^2}\left(-2\frac{\Delta x_i}{\Delta t_i} + x_i' + x_{i+1}'\right)$	(2.5)
$a_{2x} = \frac{1}{\Delta t_i}\left(3\frac{\Delta x_i}{\Delta t_i} - 2x_i' - x_{i+1}'\right)$	(2.6)
$a_{1x} = x_i'$	(2.7)
$a_{0x} = x_i$	(2.8)
$a_{3y} = \frac{1}{\Delta t_i^2}\left(-2\frac{\Delta y_i}{\Delta t_i} + y_i' + y_{i+1}'\right)$	(2.9)
$a_{2y} = \frac{1}{\Delta t_i}\left(3\frac{\Delta y_i}{\Delta t_i} - 2y_i' - y_{i+1}'\right)$	(2.10)
$a_{1y} = y_i'$	(2.11)
$a_{0y} = y_i$	(2.12)

With:

$\Delta x = x_i - x_{i-1}$	(2.13)
$\Delta y = y_i - y_{i-1}$	(2.14)
$x' = \frac{\delta x}{\delta t}$	(2.15)
$y' = \frac{\delta y}{\delta t}$	(2.16)

The unknown derivatives x' and y' can be calculated by using a linear system of equations. To solve the system boundary conditions are required. The boundary areas of a butt weld or filled weld profile are even plates which means that the curvature can be assumed as zero. The impact of the boundary conditions is very small with a high amount of data points [32]. That means that the boundary conditions affect only the boundary areas. Measured areas should lay outside this area to avoid incorrect measurements. With the boundary conditions the coefficient matrix can be written as follows:

$$A = \begin{bmatrix} 2\frac{1}{\Delta t_1} & \frac{1}{\Delta t_1} & & & \\ \frac{1}{\Delta t_1} & 2\left(\frac{1}{\Delta t_1}+2\frac{1}{\Delta t_2}\right) & \frac{1}{\Delta t_3} & & \\ & \ddots & \ddots & \ddots & \\ & & \frac{1}{\Delta t_{n-1}} & 2\left(\frac{1}{\Delta t_{n-1}}+2\frac{1}{\Delta t_n}\right) & \frac{1}{\Delta t_n} \\ & & & \frac{1}{\Delta t_n} & 2\frac{1}{\Delta t_n} \end{bmatrix} \quad (2.17)$$

The linear system of equations needs to be solved for x' and y':

$$A \cdot \begin{bmatrix} x_1' \\ x_2' \\ \vdots \\ x_{n-1}' \\ x_n' \end{bmatrix} = \begin{bmatrix} 3\frac{\Delta x_1}{\Delta t_1^2} \\ 3\frac{\Delta x_1}{\Delta t_1^2}+3\frac{\Delta x_2}{\Delta t_2^2} \\ \vdots \\ 3\frac{\Delta x_{n-2}}{\Delta t_{n-2}^2}+3\frac{\Delta x_{n-1}}{\Delta t_{n-1}^2} \\ 3\frac{\Delta x_{n-1}}{\Delta t_{n-1}^2} \end{bmatrix} \quad (2.18)$$

$$A \cdot \begin{bmatrix} y_1' \\ y_2' \\ \vdots \\ y_{n-1}' \\ y_n' \end{bmatrix} = \begin{bmatrix} 3\frac{\Delta y_1}{\Delta t_1^2} \\ 3\frac{\Delta y_1}{\Delta t_1^2}+3\frac{\Delta y_2}{\Delta t_2^2} \\ \vdots \\ 3\frac{\Delta y_{n-2}}{\Delta t_{n-2}^2}+3\frac{\Delta y_{n-1}}{\Delta t_{n-1}^2} \\ 3\frac{\Delta y_{n-1}}{\Delta t_{n-1}^2} \end{bmatrix} \quad (2.19)$$

The derivatives x' and y' describe the slope with respect to the local coordinate t. With the results the slope and curvature of the weld can be described in the global coordinate system:

$$\frac{\delta y}{\delta x} = \frac{\delta y}{\delta t}\frac{\delta t}{\delta x} \quad (2.20)$$

For the curvature the difference quotient of the slope is used:

$$\frac{\delta^2 y}{\delta x^2} = \frac{\frac{\delta y_{i+1}}{\delta x_{i+1}} - \frac{\delta y_i}{\delta x_i}}{\Delta x} \quad (2.21)$$

For the evaluation of fillet welds the contour of the stiffener is a problem because the global slope with respect to the *x* axis is infinite. To avoid a complex transformation, it is possible to

describe the slope and curvature with respect to the *y* axis which is the reciprocal of the slope and the curvature with respect to *x*.

2.3 Application to welded joints

The equations—as defined in Section 2.2—were implemented into MATLAB to describe the profiles of different weld seams. For test purposes of the spline algorithm, different weld profiles can be represented with interpolated data points.

(a) (b)

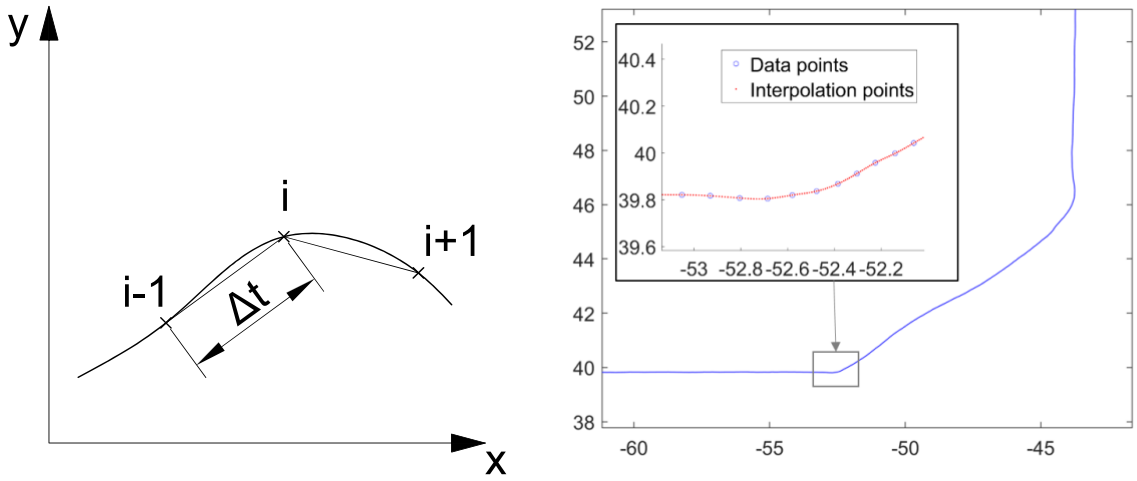

Fig. 2(b) shows a fillet weld in the as-welded condition with 10 interpolated points between each node. The fitted data points represent the profile well.

2.3.1 Measured parameters

The required main parameters are the weld radius and the weld angle. The radius at a point can be calculated by using the osculating circle [33]:

$$R = \left| \frac{\left(1 + \left(\frac{\delta y}{\delta x}\right)^2\right)^{\frac{3}{2}}}{\frac{\delta^2 y}{\delta x^2}} \right| \quad (2.22)$$

To plot the weld radius the centre coordinates are required [33]:

$$x_m = x - \frac{\frac{\delta y}{\delta x}\left(1 + \left(\frac{\delta y}{\delta x}\right)^2\right)}{\frac{\delta^2 y}{\delta x^2}} \quad (2.23)$$

$$y_m = y + \frac{1 + \left(\frac{\delta y}{\delta x}\right)^2}{\frac{\delta^2 y}{\delta x^2}}$$	(2.24)

To avoid the infinite slope areas—mentioned in Section 2.2—for the stiffener in fillet welds, the same equations can be used by replacing $\delta y/\delta x$ with $\delta x/\delta y$ and $(\delta^2 y)/(\delta x^2)$ with $(\delta^2 x)/(\delta y^2)$ without transformation.

The approach to calculate the flank angle is an independent function without an input parameter based on a tangent evaluation, see Schubnell et al. [17]. With this method the osculating circle with the centre coordinates from Eq. 2.23 and 2.24 is plotted. The circle covers some data points in the close range of the evaluation point. The last point that is covered from the circle defines the tangent point. The flank angle is the intersection angle of the two tangents. This is schematically presented in Fig. 3.

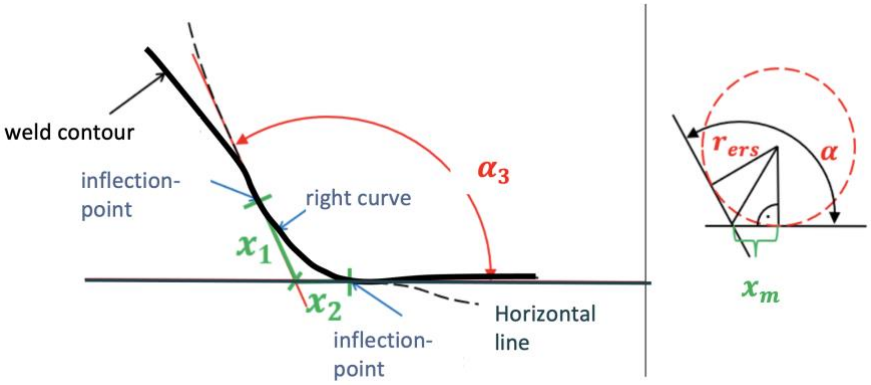

Fig. 3: Schematic presentation of the weld angle measurement technique

The main objective is to find the bottom and top weld toe. At the beginning of the measurement, the characteristic domains of the weld are identified. For our case, these are the plate, the weld, and the stiffener. For identification, the curvature of the spline—as defined in Section 2.1—is used with the Eq. 2.21. The curvature is calculated with respect to the x and y axis. As a result, four zones follow:

- Maximum curvature with respect to *x*
- Minimal curvature with respect to *x*
- Maximal curvature with respect to *y*
- Minimal curvature with respect to *y*

For the calculation of the curvature the slope is used (see Eq. 2.20). With respect to the x axis that means for the slopes:

$\left[\frac{\delta y}{\delta x}\right]_{Plate} \rightarrow 0$	(2.25)
$\left[\frac{\delta y}{\delta x}\right]_{Stiffener} \rightarrow \infty$	(2.26)

The same applies for the curvature:

$\left[\frac{\delta^2 y}{\delta x^2}\right]_{Plate} \rightarrow 0$	(2.27)
$\left[\frac{\delta^2 y}{\delta x^2}\right]_{Stiffener} \rightarrow \infty$	(2.28)

With respect to the y axis, it is the other way around. These conditions can be used to identify the plate and the stiffener domains:

- Plate: $\left[\frac{\delta y}{\delta x}\right]_{min}$ or $\left[\frac{\delta x}{\delta y}\right]_{max}$
- Stiffener: $\left[\frac{\delta y}{\delta x}\right]_{max}$ or $\left[\frac{\delta x}{\delta y}\right]_{min}$

In these domains a polynomial fit of first degree is performed. These fitted lines represent the plate and the stiffener. With the intersection point of these two lines the resulting leg length can be measured. The weld toe areas can be identified with the intersection of the leg length and the weld profile. At this point a defined search radius represents a search area for the exact weld toe. The point with the highest curvature in the search radius is the weld toe which can be evaluated.

2.3.2 Detection of incorrect measurements

After the analysis of the weld toes, it is possible to check the evaluated results of the weld radius and the weld angle. These two parameters are a good indicator whether a measurement is correct or not. An example of an incorrect measurement is an evaluation on a straight surface. The result is a high radius and an angle close to 180 degrees (see Fig. 4 (a)). Another indication of an incorrect measurement is an intersection of the plotted radius with the weld profile (see Fig. 4 (b)). In this case the plotted radius is too big and the resulting angle does not represent the weld toe. A problem like that can be identified by searching data points

in the plotted radius. A given maximum value (0.1 mm) was used to identify such an incorrect measurement.

The program automatically increases the search radius as long as the measured value exceeds the given maximum or until a given iteration limit is reached. If the iteration limit is reached without an acceptable result the measurement is marked as incorrect and the output is ignored.

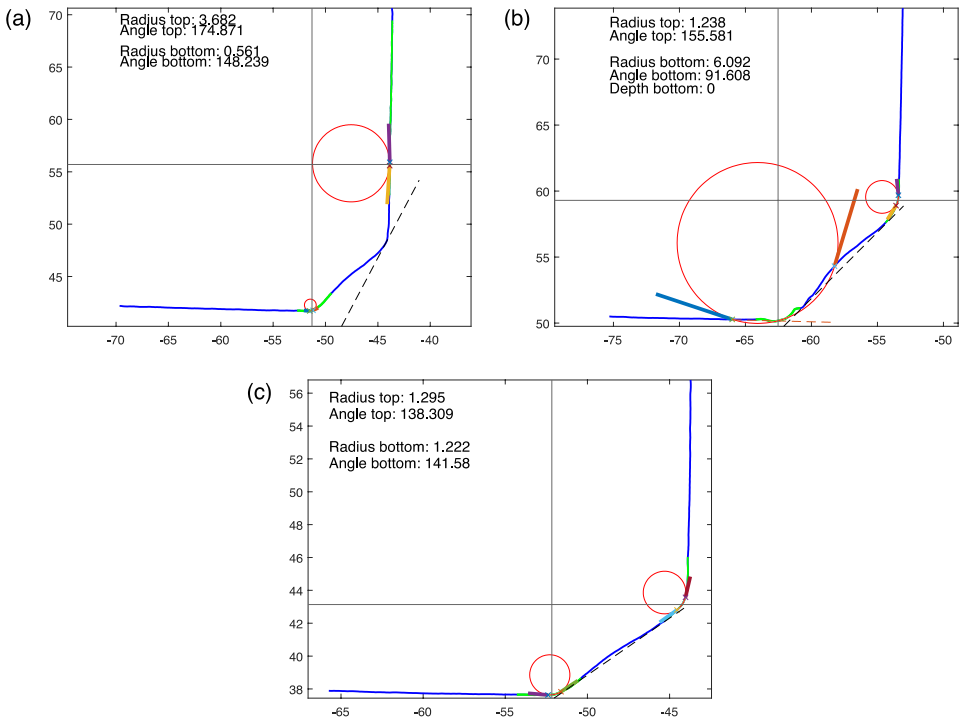

Fig. 4: Examples of incorrect measurements with measurement on a straight surface (a), Intersection of the radius and the profile (b) and a correct measurement (c)

2.3.3 ISO 5817 Evaluation

To assess the quality of the weld profiles—based on a well-established method—an evaluation according to ISO 5817:2014 [30] (with reference to ISO 6520-1 [34]) was also implemented. It is also a representative character for the fatigue strength [35]. For this, the evaluation is reduced on geometrical irregularities, see Table 1. The lengths (indicated by 'L') corresponding to these parameters can be seen in Fig. 5.

Table 1: List of included geometrical irregularities and corresponding reference numbers in ISO 5817:2014 [30] and ISO 6520-1:2007

Category	**ISO 5817:2014 [30] number**	**ISO 6520-1 [34] number**	**Quality level**		
			D	**C**	**B**
Undercut of a fillet weld	1.7	501	$h \leq 0.2 \cdot t$ Max. 1 mm	$h \leq 0.1 \cdot t$ Max. 0.5 mm	$h \leq 0.05 \cdot t$ Max. 0.5 mm
Weld reinforcement of a fillet weld	1.10	503	$h \leq 1 + 0.25 \cdot b$ Max. 5 mm	$h \leq 1 + 0.15 \cdot b$ Max. 4 mm	$h \leq 1 + 0.1 \cdot b$ Max. 3 mm
Weld angle of a fillet weld	1.12	505	$\alpha \geq 90°$	$\alpha \geq 100°$	$\alpha \geq 110°$
Asymmetric fillet weld	1.16	512	$h \leq 2 + 0.2 \cdot a$	$h \leq 2 + 0.15 \cdot a$	$h \leq 1.5 + 0.15 \cdot a$
Too small throat thickness of a fillet weld	1.20	5213	$h \leq 0.3 + 0.1 \cdot a$ Max. 2 mm	$h \leq 0.3 + 0.1 \cdot a$ Max. 1 mm	Not allowed
Too large throat thickness of a fillet weld	1.21	5214	$Allowed$	$h \leq 1 + 0.2 \cdot a$ Max. 4 mm	$h \leq 1 + 0.15 \cdot a$ Max. 3 mm
h: Limit (see category), *b*: Diagonal distance between weld toes, *a*: Throat thickness					

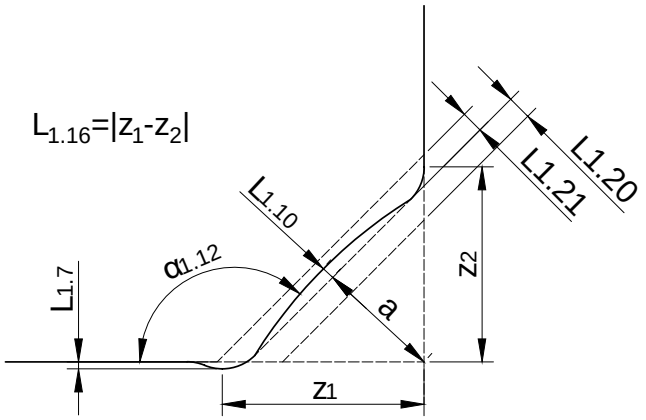

Fig. 5: ISO 5817 parameters for the quality assessment

For each irregularity the quality class B, C and D can be defined in which quality class B represents the highest quality. If the result does not fulfil the requirements of quality class D, it is marked with no classification. The classification is done for each slice of the weld seam. For the weld the lowest class defines the result for the whole weld.

2.3.4 Stress concentration factor

The stress concentration factor K_t describes the local stress increase compared to the nominal stress σ_N due to the weld toe:

$$K_t = \frac{\sigma_{max}}{\sigma_N} \quad (2.29)$$

The local weld geometry has a high impact on the stress concentration. To avoid a time-consuming FE-modelling of each local weld geometry, a calculation of K_t with empirical equations is possible [36, 37]. These approximations typically lead to a high scatter in results. An alternative way is the use of surrogate models obtained from regression or the application of artificial neural networks (ANN) [24-26, 38]. The ANN used for our application by Oswald et al. is based on 4136 linear elastic FE-simulations of parametrized design samples and has proven high accuracy compared to former existing empirical formulas as well as a significant increase of applicable parameter ranges. More information can be found in [24]. However, the evaluation is currently only possible for fillet welds in the as-welded condition (mechanical post-weld treatment is so far excluded). For the evaluation, the highest stress concentration factor along the weld is decisive. Following parameters are used for our scanned geometries: The leg length, weld toe radii and angle.

3 Experimental procedure

For evaluation, a fillet weld is tested with the measurement method introduced in Section 2.

3.1 Specimen

The specimen is a transverse stiffener made of a S235J2+N structural steel with four fillet welds and with a total number of eight different weld toes, see Braun et al. [39] for further details. Four weld toes are located at the plate (bottom) and four weld toes are located at the stiffener (top), see Fig. 1 (a). Each fillet weld is produced by a metal active gas (MAG) welding process (process number 135 according to DIN EN ISO 15614-1:2017-12 [40]). All four welds

remain in the as-welded condition. For the evaluation only one weld is used. In Fig. 1 (a) the used weld can be seen.

Plate and stiffener have a thickness of 10 mm and a length of 250 mm. For the production of the specimen no throat thickness was specified which is necessary for the ISO 5817:2014 [30] assessment. For this reason a manual measurement is conducted by using a welding gauge. All four weld seams have a throat thickness between 4 and 5 mm. A throat thickness of 4 mm is used for the quality evaluation to avoid a manipulation of the weld quality in the beginning because too a small throat thickness is not allowed for quality class B.

3.2 Specimen preparation and laser scanning

To achieve reliable results, the imported data has to represent the real geometry. This requires a good scan result which depends on the preparation of the specimen. To avoid gaps in the imported surface, a high contrast of the specimen should be prevented. A surface without contrast can be obtained by the application of a thin layer of chalk (see Fig. 1 (a)).

The input data for the evaluation derives from a laser scan, which produces a 3D point cloud composed of slices. For the following case study up to 1000 slices are generated with 512 data points per slice. This high resolution allows a good representation of the weld toes. Of each weld seam, the middle segment of 160 mm is scanned to achieve a maximum number of 1000 slices (data storage limit of the used 3D laser).

4 Statistical evaluation

Box plots represent the data on the basis of a normal distribution, see Fig. 6 for box plots for the bottom weld toe radius and angle. The centred red line is the median value and the grey box has its upper bound at the median of the upper half (Q3) of the data set and the lower bound at the median at the lower half of the data set (Q1) (see Fig. 6 (c)). Values outside the whiskers are regarded as possible outliers.

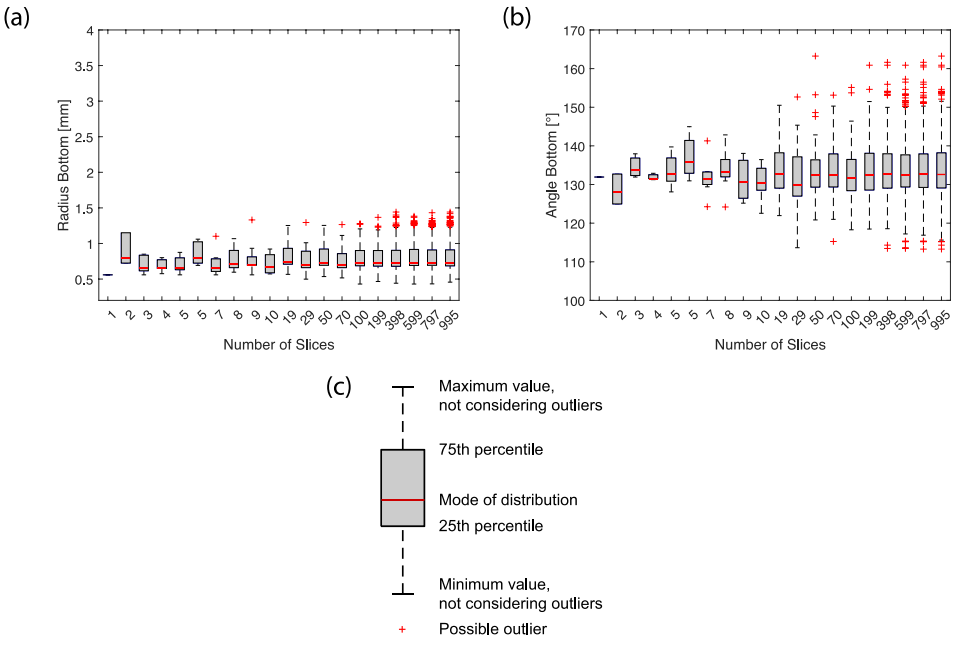

Fig. 6: Box plots of radius (a) and angle (b) at base plate weld toe for various slice numbers of specimen MAG-A-1, including boxplot legend (c)

The more the median (red line) is out-centred between Q1 and Q3 the more skewed is the distribution and a good fit of the normal distribution is less likely. This is very pronounced for the radius measurements (Fig. 6 (a)).

On the basis of the boxplots other distributions have been tested for their goodness-of-fit test (Kolmogorov-Smirnov test) for the bottom weld toe radius and angle for each of the four weld toes (numbers behind the radius und angle refer to the segment of the weld). The results of the goodness-of-fit tests are found in Table 1, where the index, 1, means that the null-hypothesis, i.e. the distribution is a good fit, is rejected, meaning that there is a statistical significant difference between the data points and the distribution [41, 42]. This means that the goodness-of-fit-test is passed when the cell is 0 and failed when it is 1. In all cases a default significance level of 5% has been used.

Table 2: Results of the goodness-of-fit test for the corresponding distributions (0 = fit test passed, 1 = fit test not passed) with and without outliers

		Parameter							
Distribution	Including possible outliers	Radius 1	Radius 2	Radius 3	Radius 4	Angle 1	Angle 2	Angle 3	Angle 4

Normal	Yes	1	0	1	1	0	0	1	0
	No	1	1	0	1	0	0	0	0
Log-normal	Yes	0	0	1	1	0	0	0	0
	No	0	0	0	0	0	0	0	0
Weibull	Yes	1	1	1	1	1	1	1	1
	No	1	1	0	1	1	1	1	1
Gamma	Yes	1	0	1	1	-	0	1	-
	No	0	0	0	0	-	0	0	-
Exponential	Yes	1	1	1	1	1	1	1	1
	No	1	1	1	1	1	1	1	1
Extreme value	Yes	1	1	1	1	1	1	1	1
	No	1	1	1	1	1	1	1	1

The results in Table 2 indicate that the log-normal is the best fit, despite the Null Hypothesis is rejected for Radius 3 and Radius 4. This agrees with results obtained by Schork et al. [11]. However, using the box-plot as a basis the data points beyond the whiskers are considered as outliers and the goodness-of-fit test is repeated. Table 2 reflects that the log-normal distribution appears to fit expectedly better without the potential outliers, which confirms the assumption of a log-normal distribution.

However, the Kolmogorov-Smirnov (KS) test can reject the hypothesis if the selected distribution fits well over most of the CPD (cumulative probability), but e.g. with large differences at upper end of the CPD. This is due to the mathematical nature of the KS test.

5 Data Analysis

For further investigations a data analysis is necessary to evaluate the parameters of a weld. With this knowledge a representative slice density (slices per length) can be determined.

An important factor for the evaluation is a reliable measurement method. The method can detect incorrect measurements (see Section 2.3.2). For a reliable assessment 1000 slices for each weld seam are generated and are measured and the reliability can be evaluated with the error rate which is the percentage of the rejected slices out of 1000. The results are presented in Table 3. It can be seen that each weld has a very low error rate (rejected assessments) which is an indicator for a reliable method. Visual inspections of all rejected slices and exemplary

measurements confirmed the results. An example for a correct measured slice is shown in Fig. 4 (c).

Table 3: Error rate of the measurement method

Weld name	Number of rejected slices bottom	Number of rejected slices top	Error rate bottom [%]	Error rate top [%]
MAG-A-1	5	10	0.5	1.0
MAG-A-2	3	15	0.3	1.5
MAG-A-3	6	6	0.6	0.6
MAG-A-4	7	5	0.7	0.5

5.1 Measurement Results

Since the measurement method proofs its reliability, it can be used on the given welds. The important weld parameters are the weld toe parameters which are the radius and the angle. With these parameters an evaluation of the stress concentration factor is possible. To conduct a quality analysis of the weld, an assessment regarding ISO 5817:2014 [30] is carried out.

Each weld is divided into a specific number of slices. Also, a new parameter of the slice density is used. The parameter represents the slices per millimetre and is made independent of the weld length by dividing the weld length by the chosen number of slices.

5.1.1 Weld parameters and stress concentration factor

Subsequently, the effect of number of slices and slice density is exemplarily investigated for the bottom weld toes (between base plate and weld flank). For the evaluation the modal value is used which represents the value that is most likely to occur. The modal value (most frequent value of the data-set, distribution peak) of the radius and angle can be plotted with respect to the slice number and the slice density (see Fig. 7 (a) and (b)). It can be observed that for the lower slice numbers a comparable value cannot be reached because the variation of the modal value is too high.

The same approach can be used for the stress concentration factors. For the evaluation of stress concentration factors with respect to the approach in [24] the parameter range is as follows:

- Radius: 0.1 mm – 2.5 mm
- Angle: 110° – 160°
- Leg length: 3 mm – 20 mm

Fig. 6 shows the majority of the weld toe radii and the angle fulfil the requirements. Out of 1000 slices the weld leg length lies between 3.5 mm and 10 mm which also fits the parameter range.

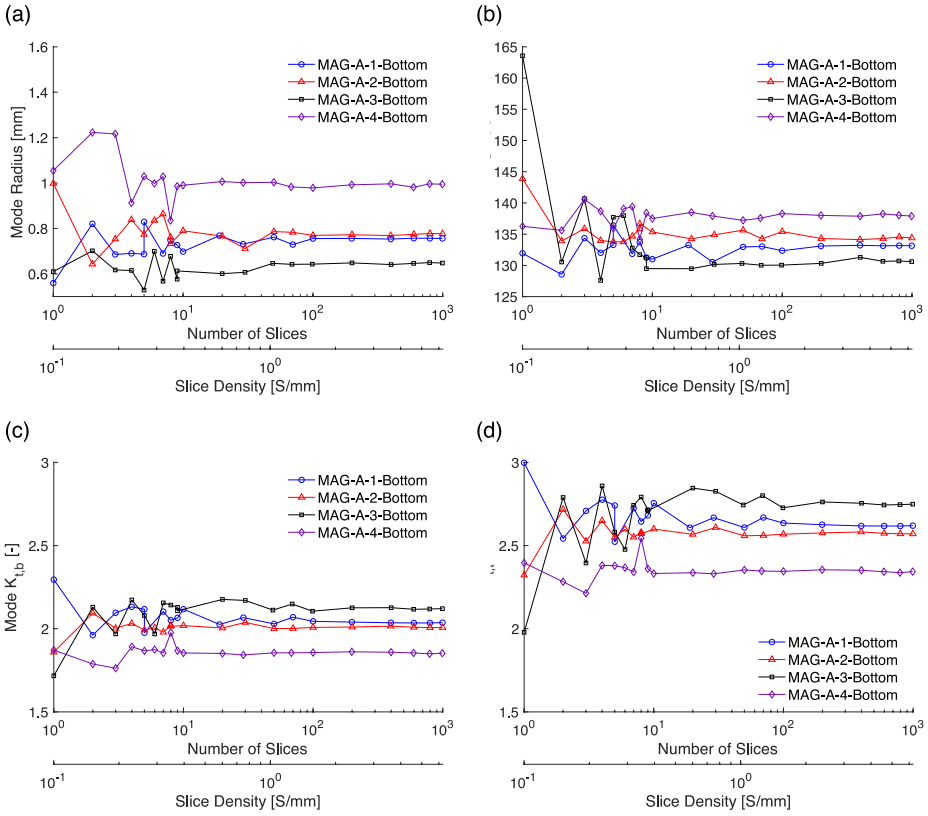

Fig. 7: Modal values of the weld parameters: radius (a) angle (b), stress concentration factor for bending (c) and tension loading (d) with respect to the number of slices and slice density

With the parameters in the given range an evaluation of the stress concentration factors for bending ($K_{t,b}$) and tension ($K_{t,t}$) is possible. For a better representation the modal value of the stress concentration factor can also be plotted with respect to the slice number and slice density for the bottom and the top weld toe (see Fig. 7 (c) and (d). The scatter of the modal value of the stress concentration factors also clearly decreases with higher slice density.

5.1.2 ISO 5817

An evaluation regarding ISO 5817:2014 [30] is conducted for every number of slices. The fillet welds are tested with the in Section 2.3.3 presented categories. The last two categories are considered as one category because the throat thickness is either too high or too low. If the weld seam has areas with too small and too high throat thicknesses it has results in both categories and, by extension, the worst class result counts.

For each class a plot with the corresponding slice number is plotted in Fig. 8. The horizontal lines show the transition to each class. Each area above these lines gives the ISO 5817:2014 [30] quality class of the weld.

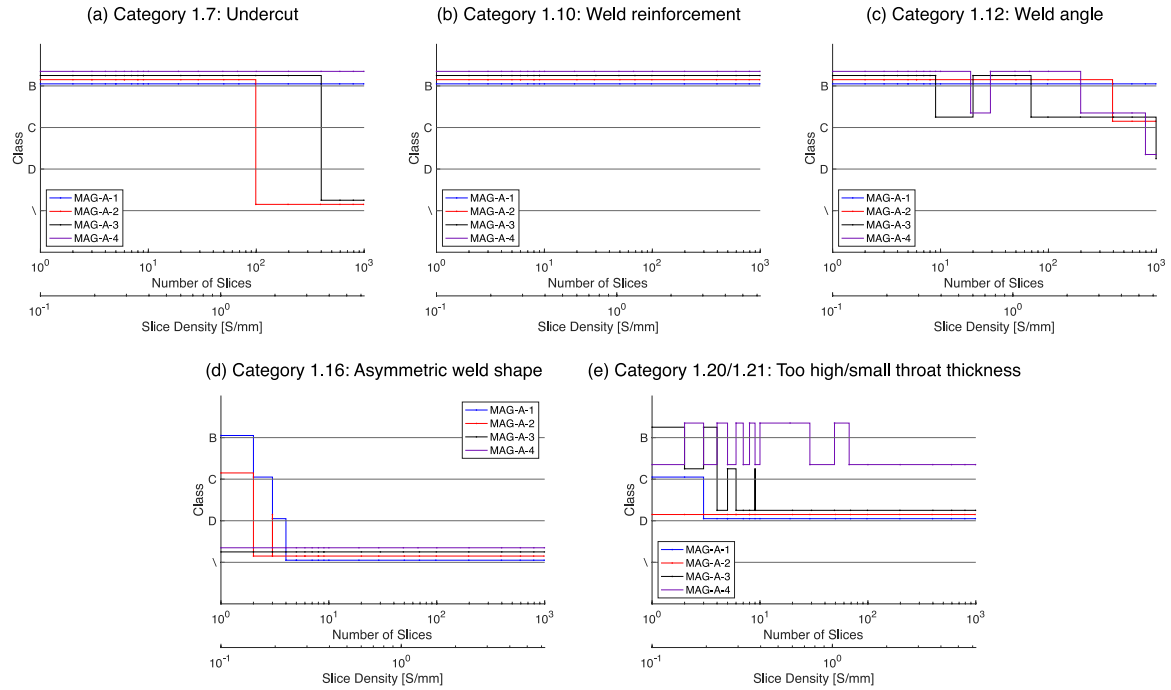

Fig. 8: Quality results for each category of ISO 5817:2014 [30]

Fig. 8 (a) shows the evaluation of the undercut (category 1.7). For a lower number of slices the best category B can be observed. With a higher number of slices the quality drops down and is even worse than the quality class D. Category 1.10 (see Fig. 8 (b)) respects the weld reinforcement. Each specimen has such a low weld reinforcement that quality class B applies. The class for the weld angle in Fig. 8 (c) (category 1.12) decreases with higher slices from class B to class D for four specimens. Fig. 8 (d) shows a low quality in category 1.16 which indicates an asymmetric weld. The asymmetric shape can be seen in Fig. 4 (c). In Fig. 8 the deviation of the aimed throat thickness is presented. The quality class lays between class B and D.

5.2 Determination of the slice number/density

For the evaluation of a weld seam, it is necessary to determine the results with an adequate number of slices. Too low slice numbers show a high scatter in the data which leads to inconsistent results. Very high slice numbers produce more reliable results but this approach needs much more calculation time. For this reason, a minimum slice number needs to be evaluated. The slice number is a factor which is affected by the weld length. Due to this reason the slice density (slices per length) is used because it is independent of the weld dimensions.

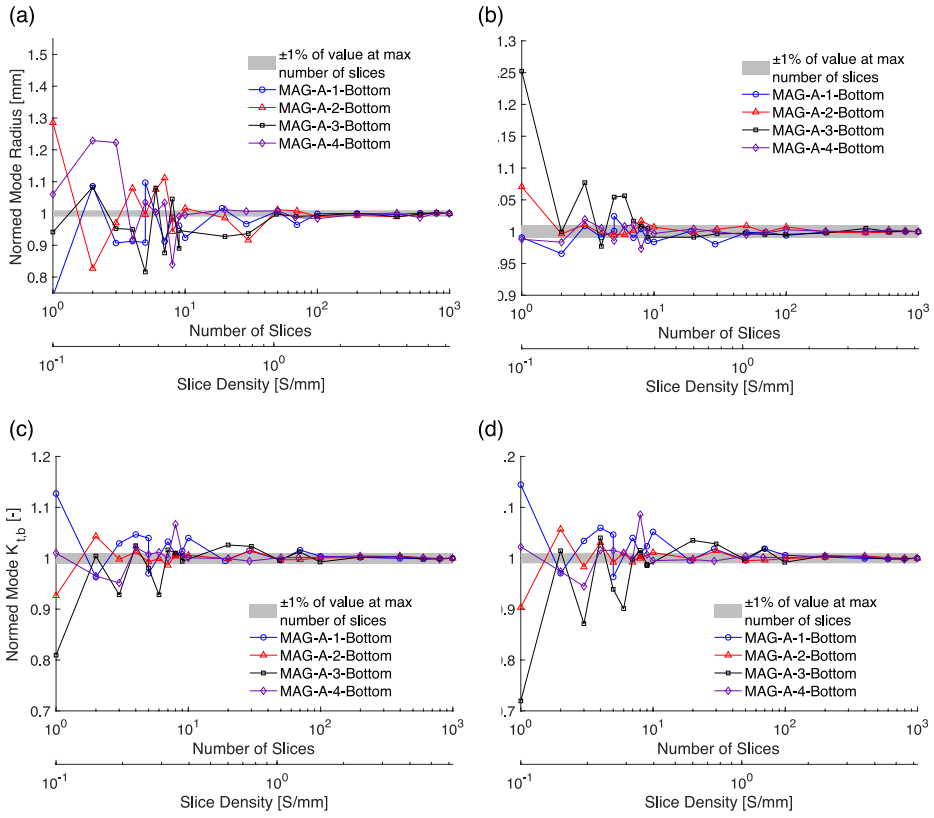

Fig. 9: Normalized weld parameters and normalized stress concentration factors with respect to the number of slices and slice density

To calculate the minimal slice density, it is necessary to identify the point where the values become nearly constant. For this reason, the values in Fig. 9 are normalized with the value of the maximal slice number. A nearly constant value is reached when the difference between this value and the value at maximal number of slices is not greater than ± 1 %. The results can be seen in Fig. 9 (a) to (b) for the weld parameters and in Fig. 9 (c) to (d) for the stress concentration factors. Fig. 9 shows that the values reach the ± 1% area at 200 slices which equals a slice density of 1.25 S/mm.

6 Comparison between small-scale specimens and long weld seams

To assess whether small-scale specimens are representative for long weld seams, a comparison between a long weld and a specific number of smaller specimens is conducted. A representative evaluation is performed for the bottom weld toe MAG-A-1 because it has the lowest scatter, see Fig. 9.

To compare the smaller specimens with the long weld, the total weld length of 160 mm is separated into four specimens with a length of 40 mm—typical for small-scale specimens. Thus, it is possible to investigate the comparability of small-scale specimens which are used for fatigue testing with a real weld. The weld seam does not contain a start or stop section. For a reliable result the slice density should be at least 1.25 S/mm (see Section 5.2). In this approach a higher slice density is used. The long weld is separated into 800 slices which results into 200 slices for each specimen. With this arrangement a slice density of 5 S/mm is achieved. The distribution of the radius, the angle, the leg length, stress concentration factor for bending and for tension are presented in Fig. 10(a).

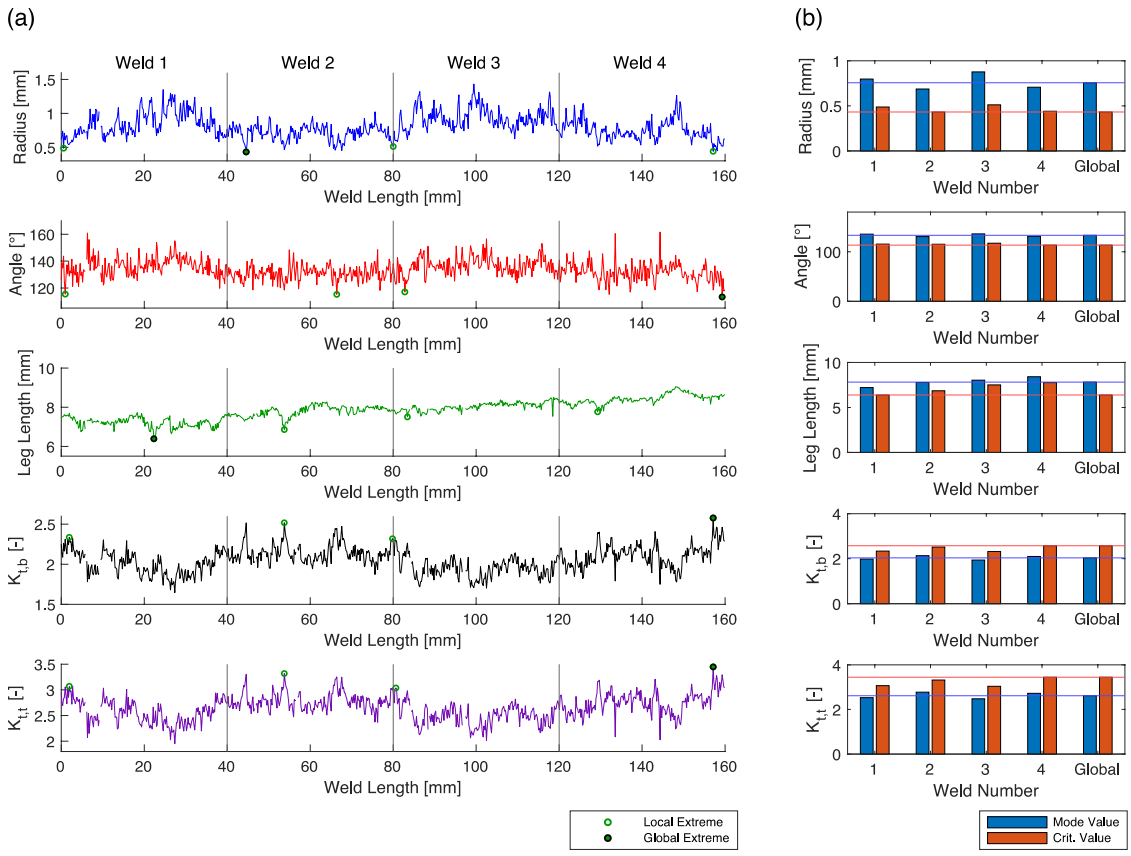

Fig. 10: Distribution of the radius, angle, leg length a stress concentrations factors for a 160 mm long weld separated into four 40 mm segments representing four specimens

It can be seen that each value has a high scatter along the weld length. The shape of the both K_t factors are nearly identical and differs only in the magnitude. Also, the impact of the radius and the angle on stress concentration can be seen. With higher radius and angle, the consequence is a lower stress concentration. Compared to the other parameters, the scatter of the weld angle and the leg length is low. Due to the high scatter of the other parameters the results for each specimen differs. To differentiate the results, the modal value and the most critical parameters of each specimen are compared with the results of the complete weld. The results are plotted as bar plot in Fig. 10(b) which allows the comparison with the global weld.

Especially the modal value of the radius is clearly above the max value. The reason for that are high magnitudes of the radius in both directions. This differences between the magnitudes are not so high for the other parameters. However, in all cases the modal value cannot match the critical values.

In order to classify the quality of the weld an evaluation of the ISO 5817:2014 [30] along the weld is conducted. The evaluation of each slice is conducted in the categories 1.7, 1.10, 1.12, 1.16 and 1.21. Because the weld seam has not a too small throat thickness, category 1.20 is not considered. The results for each slice are plotted along the weld in Fig. 11.

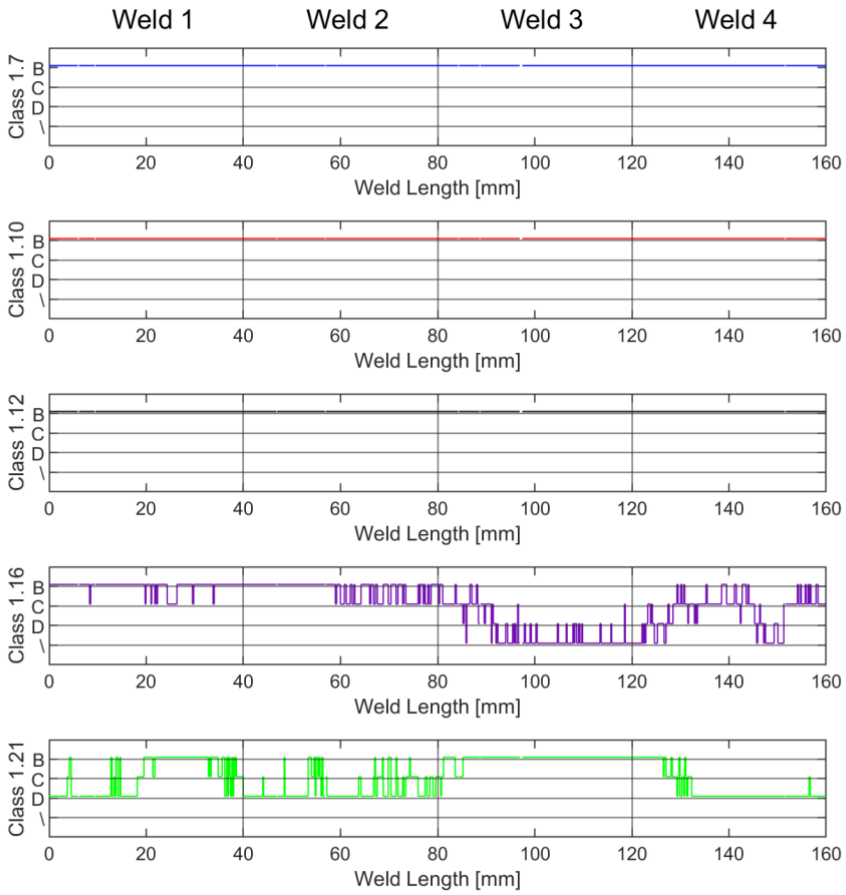

Fig. 11: Weld quality along the weld according to ISO 5817:2014 [30]

The categories 1.7, 1.10 and 1.12 have the highest quality along the complete weld. However, the categories 1.16 and 1.21 show different classes along the weld. Based on class 1.16 it can be seen that the weld is asymmetric in the second half while it is not the case in the first half. The throat thickness differs in the range of the first two specimen. The problem is caused by the manual welding torch, which leads to a deviation of the weld shape.

7 Summary and discussion

A measurement method was devolved and used for a statistical evaluation of the weld toe parameters and the weld quality, and subsequently applied to a filled-weld. A comparison of small-scale specimens with a long weld seam was carried out. The evaluated parameters were

the weld toe radius, the weld toe angle and the stress concentration factor. Furthermore, an assessment of the weld quality was conducted with respect to the ISO 5817:2014 [30] standard.

The radius or the angle alone cannot describe the quality or fatigue performance of a weld. A better parameter for that is the stress concentration factor which takes the geometry and the loading condition (tension or bending) into account. Overall, four weld segments with bottom and the top weld toes were scanned and evaluated.

The weld quality classification (according to ISO 5817:2014 [30]), showed a strong slice density dependence. A constant quality for all specimen along all evaluated slice numbers was only achieved in category 1.10. In the other cases the quality decreased with higher slice density, e.g. for the undercut depth criterium (category 1.7). All weld seams fulfilled class B for less than 200 slices. Then two weld seams dropped from the best quality to the worst.

The weld quality along the weld demonstrated that category 1.7, 1.10, and 1.12 showed the same quality along the whole weld. For category 1.16 a decrease in quality was seen for weld 3. The quality dropped from B to under the conditions of class D due to an asymmetric weld shape. However, the throat thickness which is evaluated in category 1.21 showed the best quality for weld 3. This means that a comparable result between the specimen and the global weld is not possible for category 1.16 and 1.21 in this case.

The long weld seam was separated into four welds with a length of 40 mm each and the bottom weld toe was exemplarily assessed. Due to the low error rate and the low scatter of parameters the fillet weld MAG-A-1 condition was used.

The course of the parameters for the long weld with four separated sections which represents small-scale specimens showed a similar value of $K_{t,b}$ and $K_{t,t}$. That became clear by the consideration of the global and local extreme values. Compared to the radius, the angle had a lower scatter along the weld. To compare the scatter, it is meaningful to compare normalised parameters (see Fig. 12). The parameters are each normalised by the corresponding modal value. Fig. 12 shows a high scatter for the radius compared to the other parameters. The lowest scatter is observed for the angle. Both stress concentration factors have a similar scatter; however, the scatter for the bending case is slightly larger.

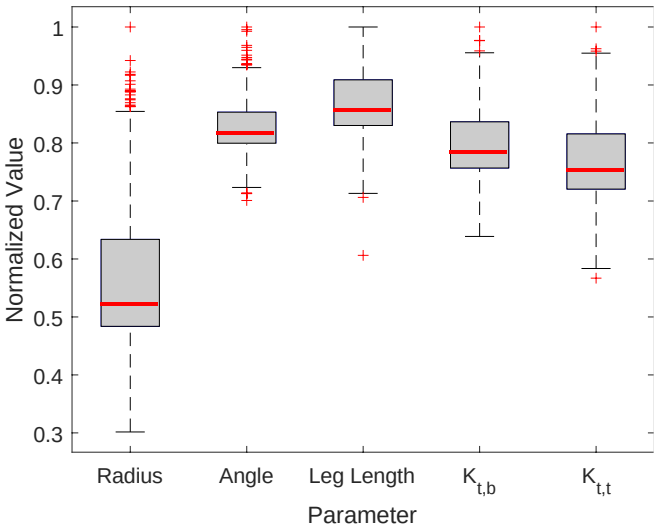

Fig. 12: Scatter of the normalised data normalised by the corresponding modal value

The comparison of the modal value and the most critical value showed a wide difference between the mode and the critical value especially for the radius. That was due to the high scatter in the data for the radius and the skewed distribution. The angle with the lower scatter in the data had nearly the same mode and critical value for each weld. Similar results were observed for both K_t values. In all cases, except for the radius, it was possible to deduce the modal value of the individual specimen to the modal value of the entire weld. The critical values, however, only fitted for the angle. In all other cases weld number 1 and 3 showed deviations from the global value while the other two specimens showed comparable results.

It should be noted that the modal value does not represent a conservative value. Therefore, the critical value is clearly the better parameter, because the weld tends to the crack initiation at the most critical location [27]. The critical stress concentration factors are the most suitable parameters compared to the other geometrical parameters to describe the fatigue performance along a weld seam because it combines the measured parameters [24, 25]. A problematic aspect of the critical value is that this value is only meaningful when all slices are taken into account. Only then it is secured that the most critical value is part of the evaluated data. With a lower slice density, the most critical slice could lie in an unassessed area. Also, due to the differences between the local and the global weld it is not possible to conclude the fatigue of the whole weld based on the fatigue strength of a single specimen. In all cases, except for the leg length, weld 4 had the most critical results, which defined the global results. This disagree with the results in [23] where the leg length had the largest contribution for the

crack initiation while the radius had less contribution. However, no actual fatigue tests were performed on the here presented specimen.

In order to expand this investigation, the contribution of each parameter to the stress concentration factors are compared. In Fig. 13 the normalised three input parameters weld radius, weld angle and leg length are shown. To ease comparison, the reciprocal values of the stress concentration factors are shown in Fig. 13 since these become maximum for small input parameters. Next, the five largest maxima are marked with circles.

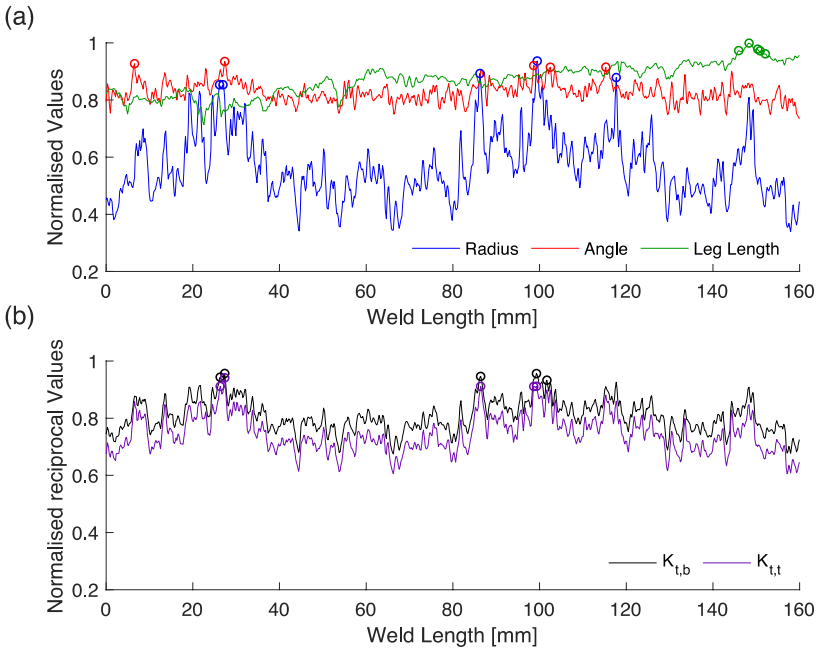

Fig. 13: Normalised values along the weld seam with the five highest maximums for geometrical features (a) and stress concentration factors for tension and bending loading (b)

It can be seen that the radius clearly affects the location of maximum stress concentration factors, because the peaks are in the same area. The leg length increases along the weld. However, this does not seem to affect the stress concentration factors.

8 Conclusion

A statistical evaluation of the weld parameters and the weld quality along the weld seam was conducted for a fillet-weld in as-welded condition. For the measurement and the quality assessment an algorithm was developed to determine the necessary slice density which is needed for a reliable and repeatable representation of the weld seam. With the gained

knowledge a comparison of smaller specimens with the global weld was conducted. The following observations and conclusions are made:

- The usage of a slice density of 1.25 slices per millimetre leads to representative results for the weld toe parameters and the stress concentration factors of the long weld seam and the four segments (representing small-scale specimens). This information permits a determination of the minimum slices number required for a representative geometric description of weld seams.
- A statistical evaluation supported the assumption of log normal distributed weld parameters (weld toe radius and angle).
- With more slices the quality according to ISO 5817:2014 [30] reduced because the probability of the existence of a slice with a lower quality increased.
- Comparable results between single specimens and the global weld are only valid for the modal value of the weld parameters. The critical value showed differences between the single specimens which resulted in different parameters for each specimen. This can affect the fatigue strength.
- To evaluate the fatigue strength the modal value is not conservative. The better option is the critical value. This value is only usable if all critical areas (or an agreed-upon quantile of the critical value) of the weld are respected by determining a suitable slice density. Assuming that the most critical slice determines the fatigue strength, the most critical specimen is representative for a longer weld seam. This should be further investigated.
- For the assessment of the fatigue performance along a weld seam the highest stress concentration factor is the most suitable parameter because it combines different weld geometry parameters.
- The stress concentration factors were mostly affected by the radius and the angle. Only a minor effect of the leg length was observed.

With the developed algorithm it is possible to measure different weld geometries with a quality evaluation with respect to ISO 5817:2014 [30]. Based on the measured data a statistical evaluation was conducted. The method worked very reliable for fillet welds in as-welded condition which can be seen in the low error rate of the evaluation.

References

[1] W. Fricke, Recent developments and future challenges in fatigue strength assessment of welded joints. Proceedings of the Institution of Mechanical Engineers, Part C: Journal of Mechanical Engineering Science, 229 (2014) 1224-1239. https://doi.org/10.1177/0954406214550015
[2] B. Schork, U. Zerbst, Y. Kiyak, M. Kaffenberger, M. Madia, M. Oechsner, Effect of the parameters of weld toe geometry on the FAT class as obtained by means of fracture mechanics-based simulations. Welding in the World, 64 (2020) 925-936. https://doi.org/10.1007/s40194-020-00874-7
[3] B. Möller, R. Wagener, J. Hrabowski, T. Ummenhofer, T. Melz, Fatigue Life of Welded High-strength Steels under Gaussian Loads. Procedia Engineering, 101 (2015) 293-301. https://doi.org/10.1016/j.proeng.2015.02.035
[4] M.J. Ottersböck, M. Leitner, M. Stoschka, W. Maurer, Effect of Weld Defects on the Fatigue Strength of Ultra High-strength Steels. Procedia Engineering, 160 (2016) 214-222. https://doi.org/10.1016/j.proeng.2016.08.883
[5] T. Holmstrand, N. Mrdjanov, Z. Barsoum, E. Åstrand, Fatigue life assessment of improved joints welded with alternative welding techniques. Engineering Failure Analysis, 42 (2014) 10–21. https://doi.org/10.1016/j.engfailanal.2014.03.012
[6] M. Braun, A. Kahl, T. Willems, M. Seidel, C. Fischer, S. Ehlers, Guidance for material selection based on static and dynamic mechanical properties at sub-zero temperatures. Journal of Offshore Mechanics and Arctic Engineering, (2020) 1-45. https://doi.org/10.1115/1.4049252
[7] E. Harati, L. Karlsson, L.E. Svensson, K. Dalaei, The relative effects of residual stresses and weld toe geometry on fatigue life of weldments. International Journal of Fatigue, 77 (2015) 160-165. https://doi.org/10.1016/j.ijfatigue.2015.03.023
[8] B. Jonsson, J. Samuelsson, G.B. Marquis, Development of Weld Quality Criteria Based on Fatigue Performance. Welding in the World, 55 (2013) 79-88. https://doi.org/10.1007/bf03321545
[9] Z. Barsoum, B. Jonsson, Influence of weld quality on the fatigue strength in seam welds. Engineering Failure Analysis, 18 (2011) 971-979. https://doi.org/10.1016/j.engfailanal.2010.12.001
[10] S. Liinalampi, H. Remes, P. Lehto, I. Lillemae, J. Romanoff, D. Porter, Fatigue strength analysis of laser-hybrid welds in thin plate considering weld geometry in microscale. International Journal of Fatigue, 87 (2016) 143-152. https://doi.org/10.1016/j.ijfatigue.2016.01.019
[11] B. Schork, P. Kucharczyk, M. Madia, U. Zerbst, J. Hensel, J. Bernhard, D. Tchuindjang, M. Kaffenberger, M. Oechsner, The effect of the local and global weld geometry as well as material defects on crack initiation and fatigue strength. Eng Fract Mech, 198 (2018) 103-122. https://doi.org/10.1016/j.engfracmech.2017.07.001
[12] H.P. Lieurade, I. Huther, F. Lefebvre, Effect of Weld Quality and Postweld Improvement Techniques on the Fatigue Resistance of Extra High Strength Steels. Welding in the World, 52 (2008) 106-115. https://doi.org/10.1007/BF03266658
[13] T. Shiozaki, N. Yamaguchi, Y. Tamai, J. Hiramoto, K. Ogawa, Effect of weld toe geometry on fatigue life of lap fillet welded ultra-high strength steel joints. International Journal of Fatigue, 116 (2018) 409-420. https://doi.org/10.1016/j.ijfatigue.2018.06.050
[14] A. Ahola, A. Muikku, M. Braun, T. Björk, Fatigue strength assessment of ground fillet-welded joints using 4R method. International Journal of Fatigue, 142 (2021). https://doi.org/10.1016/j.ijfatigue.2020.105916
[15] P. Hammersberg, H. Olsson, Statistical evaluation of welding quality in production. Proceedings of the Swedish Conference on Light Weight Optimized Welded Structures, Borlänge, Sweden. (2010).
[16] T. Stenberg, E. Lindgren, Z. Barsoum, Development of an algorithm for quality inspection of welded structures. 2012, pp. 1033–1041.
[17] J. Schubnell, M. Jung, C.H. Le, M. Farajian, M. Braun, S. Ehlers, W. Fricke, M. Garcia, A. Nussbaumer, J. Baumgartner, Influence of the optical measurement technique and evaluation approach on the determination of local weld geometry parameters for different weld types. Welding in the World, 64 (2020) 301-316. https://doi.org/10.1007/s40194-019-00830-0

[18] C.Y. Hou, Fatigue analysis of welded joints with the aid of real three-dimensional weld toe geometry. International Journal of Fatigue, 29 (2007) 772-785. https://doi.org/10.1016/j.ijfatigue.2006.06.007
[19] A. Niederwanger, D.H. Warner, G. Lener, The Utility of Laser Scanning Welds for Improving Fatigue Assessment. International Journal of Fatigue, 140 (2020). https://doi.org/10.1016/j.ijfatigue.2020.105810
[20] T. Lassen, The Effect of the Welding Process on the Fatigue Crack Growth. Welding Journal, 69 (1990) 75–82
[21] T.J. Nykänen, G. Marquis, T. Björk, Effect of weld geometry on the fatigue strength of fillet welded cruciform joints. Proceedings of the International Symposium on Integrated Design and Manufacturing of Welded Structures, (2007).
[22] T.N. Nguyen, M.A. Wahab, A Theoretical-Study of the Effect of Weld Geometry Parameters on Fatigue-Crack Propagation Life. Eng Fract Mech, 51 (1995) 1-18. https://doi.org/10.1016/0013-7944(94)00241-9
[23] G. Hultgren, Z. Barsoum, Fatigue assessment in welded joints based on geometrical variations measured by laser scanning. Welding in the World, 64 (2020) 1825-1831. https://doi.org/10.1007/s40194-020-00962-8
[24] M. Oswald, C. Mayr, K. Rother, Determination of notch factors for welded cruciform joints based on numerical analysis and metamodeling. Welding in the World, 63 (2019) 1339-1354. https://doi.org/10.1007/s40194-019-00751-y
[25] M. Oswald, J. Neuhäusler, K. Rother, Determination of notch factors for welded butt joints based on numerical analysis and metamodeling. Welding in the World, 64 (2020) 2053-2074. https://doi.org/10.1007/s40194-020-00982-4
[26] M. Oswald, S. Springl, K. Rother, Determination of notch factors for welded T-joints based on numerical analysis and metamodeling. International Institute of Welding IIW-Doc XIII-2853-2020 (2020).
[27] M.M. Alam, Z. Barsoum, P. Jonsen, A.F.H. Kaplan, H.A. Haggblad, The influence of surface geometry and topography on the fatigue cracking behaviour of laser hybrid welded eccentric fillet joints. Applied Surface Science, 256 (2010) 1936-1945. https://doi.org/10.1016/j.apsusc.2009.10.041
[28] A. Deinböck, A.-C. Hesse, M. Wächter, J. Hensel, A. Esderts, K. Dilger, Increased accuracy of calculated fatigue resistance of welds through consideration of the statistical size effect within the notch stress concept. Welding in the World, 64 (2020) 1725-1736. https://doi.org/10.1007/s40194-020-00950-y
[29] U. Dilthey, Schweißtechnische Fertigungsverfahren 1: Schweiß-und Schneidtechnologien. Springer, 2006.
[30] EN ISO 5817:2014 Welding - Fusion welded joints in steel, nickel, titanium and their alloys (beam welding excluded) - Quality levels for imperfections. British Standards Institute (BSI), (2014).
[31] M. Jung, Development and Implementing an Algorithm for Approximation and Evaluation of Stress Concentration Factors of Fillet Welds Based on Contactless 3D Measurement. Karlsruher Institut für Technologie, Karlsruhe, Germany, 2018.
[32] A. Busch, Vergleich verschiedener linearer Algorithmen für Spline-Kurven. Schriftenreihe Schiffbau, Entwerfen von Schiffen und Schiffssicherheit M-6, 1990.
[33] G. Merzinger, G. Mühlbach, D. Wille, T. Wirth, Formeln + Hilfen Höhere Mathematik. Binomi Verlag, 2010.
[34] EN ISO 6520-1:2007 Welding and allied processes – Classification of geometric imperfections in metallic materials – Part 1: Fusion welding. British Standards Institute (BSI), (2007).
[35] B. Jonsson, G. Dobmann, A.F. Hobbacher, M. Kassner, G.B. Marquis, IIW guidelines on weld quality in relationship to fatigue strength. Springer, 2016.
[36] H. Remes, Strain-based approach to fatigue strength assessment of laser-welded joints. 2008.
[37] D. Radaj, Zur vereinfachten Darstellung der mehrparametrigen Formzahlabhängigkeit. Konstruktion, 38 (1986) 193–197

[38] M. Dabiri, M. Ghafouri, H.R. Rohani Raftar, T. Björk, Utilizing artificial neural networks for stress concentration factor calculation in butt welds. Journal of Constructional Steel Research, 138 (2017) 488-498. https://doi.org/10.1016/j.jcsr.2017.08.009
[39] M. Braun, R. Scheffer, W. Fricke, S. Ehlers, Fatigue strength of fillet-welded joints at subzero temperatures. Fatigue Fract Eng M, 43 (2020) 403-416. https://doi.org/10.1111/ffe.13163
[40] EN ISO 15614-1:2017 + A1:2019: Specification and qualification of welding procedures for metallic materials - Welding procedure test - Part 1: Arc and gas welding of steels and arc welding of nickel and nickel alloys. (2020).
[41] R.S. Kenett, S. Zacks, D. Amberti, Modern Industrial Statistics: with applications in R, MINITAB and JMP. John Wiley & Sons, Ltd, Chichester, 2013.
[42] B. Mitchell, A Comparison of Chi-Square and Kolmogorov-Smirnov Tests. Area, 3 (1971) 237–241